

State resolved rotational excitation cross sections and rates in H_2+H_2 collisionsRenat A. Sultanov*, Dennis Guster†^a^aBusiness Computer Research Laboratory, St. Cloud State University, 2nd Floor, General Office Area, BB-252, 720 Fourth Avenue South, St Cloud, MN 56301-4498

Rotational transitions in molecular hydrogen collisions are computed. The two most recently developed potential energy surfaces for the H_2-H_2 system are used from the following works: 1) A.I. Boothroyd, P.G. Martin, W.J. Keogh, M.J. Peterson, *J. Chem. Phys.*, 116 (2002) 666, and 2) P. Diep, J.K. Johnson, *J. Chem. Phys.*, 113 (2000) 3480; *ibid.* 112, 4465. Cross sections for rotational transitions $00\rightarrow 20$, 22, 40, 42, 44 and corresponding rate coefficients are calculated using a quantum-mechanical approach. Results are compared for a wide range of kinetic temperatures $300\text{ K} \leq T \leq 3000\text{ K}$.

1. INTRODUCTION

The interaction and collision properties of hydrogen molecules, and hydrogen molecular isotopes has been of great theoretical and experimental interest for many years [1, 2, 3, 4, 5, 6, 7, 8, 9, 10, 11, 12, 13, 14, 15, 16, 17, 18, 19, 20, 21, 22, 23, 24]. Because of the low number of electrons in the H_2-H_2 system this is one of the few four-center systems for which the potential energy surface (PES) can be developed with very high precision. Therefore H_2+H_2 is a benchmark collision used for testing several dynamic methods such as: semiclassical [17], quantum-mechanical [19] or wave packet [20] studies. The system may also be useful in improving our understanding of fundamental processes in few-body molecular dynamics. Additionally, the H_2+H_2 elastic and inelastic collisions are of interest in combustion, spacecraft modeling and in clean renewable energy. Hydrogen gas, in particular, has generated much interest as a energy supplier, see for example [25].

The hydrogen molecule plays an important role in many areas of astrophysics [26, 27, 28, 29]. It is the simplest and most abundant molecule in the universe especially in giant molecular clouds. Energy transfer involving H_2 molecules governs the evolution of shock fronts [26, 27] and photodissociation regions (PDRs) in the interstellar medium. Collision-induced energy transfer between H_2 molecules and between H_2 and other atoms/molecules is related to an important astrophysical processes, which is the cooling of primordial gas and shock wave-induced heating in the interstellar media. To accurately model the thermal balance and kinetics of such important systems one needs accurate state-to-state rate constants.

It is well known, that experimental measurements of quantum state resolved cross sections and rates is a very difficult technical problem. On the other hand accurate theoretical data requires precise PESs and reliable dynamical treatment of the collision processes. The first attempt to construct a realistic full-dimensional ab initio PES for the H_2-H_2 system was done in works [10, 11], and the potential was widely used in the framework of variety of methods and computation techniques.

*sultanov@bcr1.stcloudstate.edu

†dguster@stcloudstate.edu

Because of the immense theoretical and practical benefits associated with the recent hydrogen fuel issues, the $\text{H}_2\text{--H}_2$ system has been reinvestigated and an accurate interaction potential from the first principles has been developed in work [30]. However, in this work the Diep and Johnson potential energy surface (DJ PES) was extrapolated only for the rigid rotor monomer model of $\text{H}_2\text{--H}_2$. On the other hand two extensive studies of the $\text{H}_2\text{--H}_2$ PES have been reported by Boothroyd et al., [13, 31]. In these studies the potential energies have been represented at 6101 and 48180 geometries respectively with a large basis set at the multireference configuration interaction level. The earlier 6101 points were fitted to a six dimensional many-body expansion form in work [14].

In this work we present a comparative study of the global BMKP and DJ PESs for collisions of rotationally excited H_2 molecules. The scattering cross sections and their corresponding rate coefficients are calculated using a non reactive quantum-mechanical close-coupling approach. In the next section we will shortly outline the method. Our results and discussion are presented in Section 3. Conclusions are provided in Section 4. Atomic units ($e=m_e=\hbar=1$) are used throughout this work.

2. METHOD

In this section we will briefly present the close-coupling quantum-mechanical approach we used to calculate our results, specifically the cross sections and rates in collision of a hydrogen molecule with another hydrogen molecule. The Schrödinger equation for a $ab + cd$ collision in the center of a mass frame, where ab and cd are linear rigid rotors is

$$\left(\frac{P_{\vec{R}}}{2M_{12}} + \frac{L_{\hat{r}_1}}{2\mu_1 r_1^2} + \frac{L_{\hat{r}_2}}{2\mu_2 r_2^2} + V(\vec{r}_1, \vec{r}_2, \vec{R}) \right) \Psi(\hat{r}_1, \hat{r}_2, \vec{R}) = 0. \quad (1)$$

where $P_{\vec{R}}$ is the momentum operator of the kinetic energy of the collision, \vec{R} is the collision coordinate, M_{12} is a reduced mass of the pair of two-atomic molecules (rigid rotors in this model) ab and cd : $M_{12} = (m_a + m_b)(m_c + m_d)/(m_a + m_b + m_c + m_d)$, $\mu_{1(2)}$ are reduced masses of the targets: $\mu_{1(2)} = m_{a(c)}m_{b(d)}/(m_{a(c)} + m_{b(d)})$, $\hat{r}_{1(2)}$ are the angles of orientation of rotors ab and cd , respectively, J is total angular momentum quantum number of $abcd$ system and M is its projection onto the space fixed z axis, $V(\vec{r}_1, \vec{r}_2, \vec{R})$ is the potential energy surface for the four atomic system $abcd$.

The eigenfunctions of the operators $L_{\hat{r}_{1(2)}}$ in (1) are simple spherical harmonics $Y_{j_i m_i}(\hat{r})$. To solve the equation (1) the following expansion is used [5]

$$\Psi(\hat{r}_1, \hat{r}_2, \vec{R}) = \sum_{JMj_1j_2j_{12}L} \frac{U_{j_1j_2j_{12}L}^{JM}(R)}{R} \phi_{j_1j_2j_{12}L}^{JM}(\hat{r}_1, \hat{r}_2, \vec{R}), \quad (2)$$

where channel expansion functions are

$$\phi_{j_1j_2j_{12}L}^{JM}(\hat{r}_1, \hat{r}_2, \vec{R}) = \sum_{m_1m_2m_{12}m} C_{j_1m_1j_2m_2}^{j_{12}m_{12}} C_{j_{12}m_{12}lm}^{JM} Y_{j_1m_1}(\hat{r}_1) Y_{j_2m_2}(\hat{r}_2) Y_{Lm}(\hat{R}), \quad (3)$$

here $j_1 + j_2 = j_{12}$, $j_{12} + L = J$, m_1 , m_2 , m_{12} and m are projections of j_1 , j_2 , j_{12} and L respectively.

Substitution of (2) into (1) provides a set of coupled second order differential equations for the unknown radial functions $U_{\alpha}^{JM}(R)$

$$\left(\frac{d^2}{dR^2} - \frac{L(L+1)}{R^2} + k_{\alpha}^2 \right) U_{\alpha}^{JM}(R) = 2M_{12} \sum_{\alpha'} \int \langle \phi_{\alpha}^{JM}(\hat{r}_1, \hat{r}_2, \vec{R}) | V(\vec{r}_1, \vec{r}_2, \vec{R}) | \phi_{\alpha'}^{JM}(\hat{r}_1, \hat{r}_2, \vec{R}) \rangle U_{\alpha'}^{JM}(R) d\hat{r}_1 d\hat{r}_2 d\hat{R}, \quad (4)$$

where $\alpha \equiv (j_1 j_2 j_{12} L)$. We apply the hybrid modified log-derivative-Airy propagator in the general purpose scattering program MOLSCAT [32] to solve the coupled radial equations (4). Additionally, we have tested other propagator schemes included in MOLSCAT. Our calculations revealed that other propagators can also produce quite stable results.

The log-derivative matrix is propagated to large R -intermolecular distances, since all experimentally observable quantum information about the collision is contained in the asymptotic behaviour of functions $U_\alpha^{JM}(R \rightarrow \infty)$. The numerical results are matched to the known asymptotic solution to derive the physical scattering S -matrix

$$U_\alpha^J \underset{R \rightarrow +\infty}{\sim} \delta_{\alpha\alpha'} e^{-i(k_{\alpha\alpha} R - (l\pi/2))} - \left(\frac{k_{\alpha\alpha}}{k_{\alpha\alpha'}} \right)^{1/2} S_{\alpha\alpha'}^J e^{-i(k_{\alpha\alpha'} R - (l'\pi/2))}, \quad (5)$$

where $k_{\alpha\alpha'} = 2M_{12}(E + E_\alpha - E_{\alpha'})^{1/2}$ is the channel wavenumber, $E_{\alpha(\alpha')}$ are rotational channel energies and E is the total energy in the $abcd$ system. The method was used for each partial wave until a converged cross section was obtained. It was verified that the results are converged with respect to the number of partial waves as well as the matching radius, R_{max} , for all channels included in our calculations.

Cross sections for rotational excitation and relaxation phenomena can be obtained directly from the S -matrix. In particular the cross sections for excitation from $j_1 j_2 \rightarrow j'_1 j'_2$ summed over the final $m'_1 m'_2$ and averaged over the initial $m_1 m_2$ are given by

$$\sigma(j'_1, j'_2; j_1 j_2, \epsilon) = \frac{\pi}{(2j_1 + 1)(2j_2 + 1)k_{\alpha\alpha'}} \sum_{J j_{12} j'_{12} L L'} (2J + 1) |\delta_{\alpha\alpha'} - S^J(j'_1, j'_2, j'_{12} L'; j_1, j_2, j_{12}, L; E)|^2. \quad (6)$$

The kinetic energy is $\epsilon = E - B_1 j_1(j_1 + 1) - B_2 j_2(j_2 + 1)$, where $B_{1(2)}$ are the rotation constants of rigid rotors ab and cd respectively.

The relationship between the rate coefficient $k_{j_1 j_2 \rightarrow j'_1 j'_2}(T)$ and the corresponding cross section $\sigma_{j_1 j_2 \rightarrow j'_1 j'_2}(E_{kin})$ can be obtained through the following weighted average

$$k_{j_1 j_2 \rightarrow j'_1 j'_2}(T) = \frac{8k_B T}{\pi \mu} \frac{1}{(k_B T)^2} \int_{\epsilon_s}^{\infty} \sigma_{j_1 j_2 \rightarrow j'_1 j'_2}(\epsilon) e^{-\epsilon/k_B T} \epsilon d\epsilon, \quad (7)$$

where $\epsilon = E_{total} - E_{j_1} - E_{j_2}$ is precollisional translational energy at the translational temperature T and ϵ_s is the minimum kinetic energy for the levels j_1 and j_2 to become accessible.

3. RESULTS

In this section we present our results for rotational transitions in collisions between *para/para*-hydrogen molecules:

$$H_2(j_1 = 0) + H_2(j_2 = 0) \rightarrow H_2(j'_1) + H_2(j'_2). \quad (8)$$

We apply the newest PESs from the works [30] and [31]. The first one, DJ PES, is constructed for the vibrationally averaged rigid monomer model of the H_2-H_2 system to the complete basis set limit using coupled-cluster theory with single, double and triple excitations. A four term spherical harmonics expansion model was chosen to fit the surface. It was demonstrated, that the calculated PES can reproduce the quadrupole moment to within 0.58 % and the experimental well depth to within 1 %.

The bond length was fixed at 1.449 a.u. or 0.7668 Å. DJ PES is defined by the center-of-mass intermolecular distance, R , and three angles: θ_1 and θ_2 are the plane angles and ϕ_{12} is the

relative torsional angle. The angular increment for each of the three angles defining the relative orientation of the dimers was chosen to be 30° . There are 37 unique configurations for each radial separation when the symmetry of the $\text{H}_2\text{--H}_2$ system is considered. In previous works calculating the potential a much smaller set of angular configurations designed to represent the full surface was used. The potential was calculated from only 2.0 to 10.0 Å of intermolecular (center-of-mass) separation with an increment 0.2 Å. However, near the potential minimum which is from 2.7 to 4.5 Å the grid spacing is 0.1 Å. The functional form of the potential represents an expansion on Legendre polynomials [5].

The second potential, BMKP PES, is a global six-dimensional potential energy surface for two hydrogen molecules. It was especially constructed to represent the whole interaction region of the chemical reaction dynamics of the four-atomic system and to provide an accurate as possible the van der Waals well. The ground state and a few excited-state energies were calculated. The new potential fits the van der Waals well to an accuracy within about 5% and has an rms error of 1.43 millihartree relative to the 48180 ab initio energies. For the 39064 ab initio energies that lie below twice the H_2 dissociation energy BMKP PES has an rms error of 0.95 millihartree. These rms errors are comparable to the estimated error in the ab initio energies themselves. In the six-dimensional conformation space of the four atomic system the conical intersection forms a complicated three-dimensional hypersurface. The authors of the work [31] mapped out a large portion of the locus of this conical intersection.

The BMKP PES uses cartesian coordinates to compute distances between four atoms. We have devised some fortran code, which converts spherical coordinates used in Sec. 2 to the corresponding cartesian coordinates and computes the distances between the four atoms. In all our calculations with this potential the bond length was fixed at 1.449 a.u. or 0.7668 Å as in DJ PES.

Now we will present our results for the elastic and inelastic integral cross sections and rate coefficients for the collision (8). As far as astrophysical applications are concerned, we are particularly interested in the pure rotational transitions of the H_2 molecules.

A large number of test calculations have been done to secure the convergence of the results with respect to all parameters that enter into the propagation of the Schrödinger equation (1). This includes the intermolecular distance R , the total angular momentum J of the four atomic system, N_{lv} the number of rotational levels to be included in the close coupling expansion and others (see the MOLSCAT manual [32]).

We reached convergence for the integral cross sections, $\sigma(E_{kin})$, in all considered collisions. In the case of DJ PES the propagation has been done from 2 Å to 10 Å, since this potential is defined only for the specific distances. For the BMKP PES we used $r_{min} = 1$ Å to $r_{max} = 30$ Å. We also applied a few different propagators included in the MOLSCAT program.

Table 1 represents the convergence test results with respect to J_{max} , the maximum value of the total angular momentum, for both the BMKP and DJ PESs. The calculations are limited to just three values of energy, for the simpler basis set: $j_1j_2=00$, 20 and 22, and from lowest to highest within the considered range of energies. As can be seen the results are stable for the range of kinetics energies, when J_{max} is increased from 80 to 90. In all our subsequent production calculations we use $J_{max} = 80$.

It is important to point out here, that for comparison purposes we don't include the compensating factor of 2 mentioned in [9]. However, in Fig. 2 and in our subsequent calculations of the rate coefficients, $k_{jj'}(T)$, the factor is included.

In Table 2 we include the results of our test calculations for the various rotational levels j_1j_2 included in the close coupling expansion. In these test calculations we used two basis sets: $j_1j_2=00$, 20, 22, 40, 42 with total basis set size $N_{lv} = 13$ and $j_1j_2=00$, 20, 22, 40, 42, 44, 60,

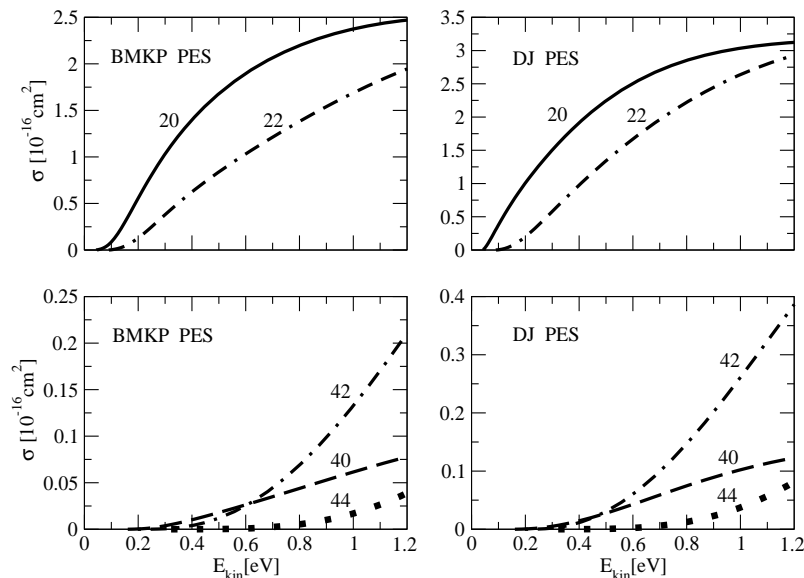


Figure 1. Rotational state resolved integral cross sections for $j_1 = j_2 = 0 \rightarrow j'_1 = 2, j'_2 = 0$, $j_1 = j_2 = 0 \rightarrow j'_1 = 2, j'_2 = 2$, $j_1 = j_2 = 0 \rightarrow j'_1 = 4, j'_2 = 0$, $j_1 = j_2 = 0 \rightarrow j'_1 = 4, j'_2 = 2$ and $j_1 = j_2 = 0 \rightarrow j'_1 = 4, j'_2 = 4$ calculated with the BMKP and DJ PESs (the compensating factor of 2 is not included).

62 with $N_{lvl} = 28$. One can see that the results are quite stable for the $00 \rightarrow 20$ and $00 \rightarrow 22$ transitions and somewhat stable for the highly excited $00 \rightarrow 40$ transition. Nonetheless, for our production calculations we used the first basis set.

The objective of this work is to make reliable quantum-mechanical calculations for different transitions in $p\text{-}H_2 + p\text{-}H_2$ collisions and provide a comparative study of the two PESs. The energy dependence of the state-resolved integral cross sections $\sigma_{j_1 j_2 \rightarrow j'_1 j'_2}(E_{kin})$ for the $j_1 = j_2 = 0 \rightarrow j'_1 = 2, j'_2 = 0$ and $j_1 = j_2 = 0 \rightarrow j'_1 = 2, j'_2 = 2$ rotational transitions are represented in Fig. 1 (upper plots) for both the BMKP and DJ PESs respectively. These channels for the most part influence the total cross-section of the $H_2 + H_2$ collision. As can be seen both PESs provide the same type of the behaviour in the cross section. These results are in basic agreement with the recent calculations of work [20], where the BMKP PES was also applied, but using a time-dependent quantum-mechanical approach. Our calculation show, that DJ PES generates higher values for the cross sections, by up to 50%.

The integral cross sections for inelastic collisions: $j_1 = j_2 = 0 \rightarrow j'_1 = 4, j'_2 = 0$, $j_1 = j_2 = 0 \rightarrow j'_1 = 4, j'_2 = 2$, and $j_1 = j_2 = 0 \rightarrow j'_1 = 4, j'_2 = 4$ for BMKP and DJ PESs are presented in Fig. 1 (bottom plots). The cross sections are very small at energies less than 0.25 eV, since at lower kinetic energies these transitions are closed by the corresponding energy barriers.

We would like to point out here, that the $j_1 = j_2 = 0 \rightarrow j'_1 = 4, j'_2 = 2$ cross section becomes larger than $j_1 = j_2 = 0 \rightarrow j'_1 = 4, j'_2 = 0$ if the collision energy is greater than ~ 0.6 eV. In this energy range it is hence more likely that the second diatom is also excited when the first diatom makes the $0 \rightarrow 4$ transition. However the $j_1 = 0, j_2 = 0 \rightarrow j'_1 = 4, j'_2 = 4$ cross section is very small over the entire energy range considered. The DJ potential energy surface again provides higher results in the corresponding cross sections. One can note, that for both potentials the

Table 1: Convergence of the total cross sections (10^{-16}cm^2) for transitions $00 \rightarrow 20$ and $00 \rightarrow 22$ with respect to the maximum value of the total angular momentum J_{max} in the $\text{H}_2\text{--H}_2$ system. Here σ_B and σ_D are the cross sections calculated with BMKP [31] and Diep and Johnson [30] PESs respectively.

E (eV)	$J_{max} = 80$				$J_{max} = 90$			
	$00 \rightarrow 20$		$00 \rightarrow 22$		$00 \rightarrow 20$		$00 \rightarrow 22$	
	σ_B	σ_D	σ_B	σ_D	σ_B	σ_D	σ_B	σ_D
1.240	2.410	3.127	2.549	3.925	2.410	3.127	2.552	3.933
0.620	1.910	2.485	1.146	1.908	1.910	2.485	1.146	1.909
0.124	1.742(-1)	5.403(-1)	1.526(-2)	2.312(-2)	1.742(-1)	5.403(-1)	1.526(-2)	2.312(-2)

Numbers in parentheses are powers of 10 (the compensating factor of 2 is not included).

Table 2: Convergence of the total cross sections (10^{-16}cm^2) for transitions from $00 \rightarrow 20, 22, 40$ with respect to the number N_{lvl} of the levels to be included in the basis set of the $\text{H}_2\text{--H}_2$ system. Here σ_B and σ_D are the cross sections calculated with BMKP [31] and Diep and Johnson [30] PESs respectively.

E (eV)	Basis set: $j_1 j_2 = 00, 20, 22, 40, 42$ ($N_{lvl} = 13$)						Basis set: $j_1 j_2 = 00, 20, 22, 40, 42, 44, 60, 62$ ($N_{lvl} = 28$)					
	$00 \rightarrow 20$		$00 \rightarrow 22$		$00 \rightarrow 40$		$00 \rightarrow 20$		$00 \rightarrow 22$		$00 \rightarrow 40$	
	σ_B	σ_D	σ_B	σ_D	σ_B	σ_D	σ_B	σ_D	σ_B	σ_D	σ_B	σ_D
1.240	2.50	3.14	1.97	3.00	7.32(-2)	1.18(-1)	2.48	3.13	1.99	2.97	8.07(-2)	1.26(-1)
0.620	1.94	2.55	1.07	1.73	2.72(-2)	4.38(-2)	1.93	2.55	1.07	1.73	2.80(-2)	4.59(-2)
0.124	1.75(-1)	5.45(-1)	1.54(-2)	2.32(-2)	0.0	0.0	1.75(-1)	5.44(-1)	1.54(-2)	2.32(-2)	0.0	0.0

Numbers in parentheses are powers of 10 (the compensating factor of 2 is not included).

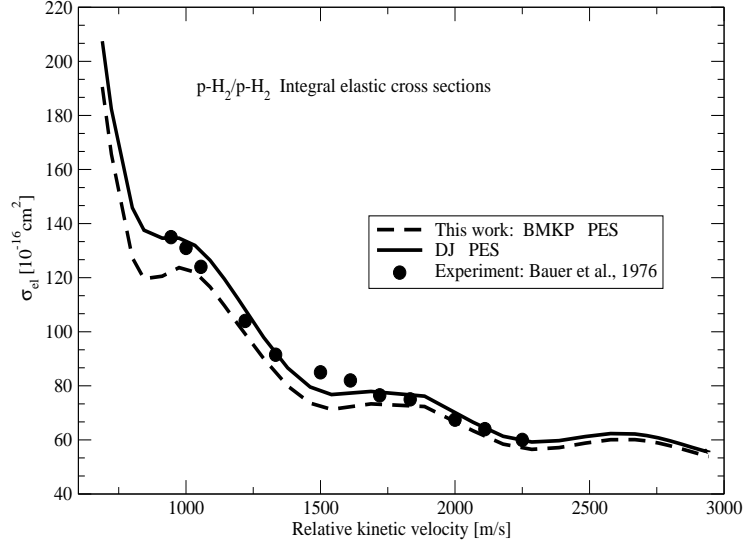


Figure 2. Integral elastic cross sections calculated with the BMKP and DJ potentials. The experimental measurements are those of Bauer and co-workers [6] (the compensating factor of 2 is included).

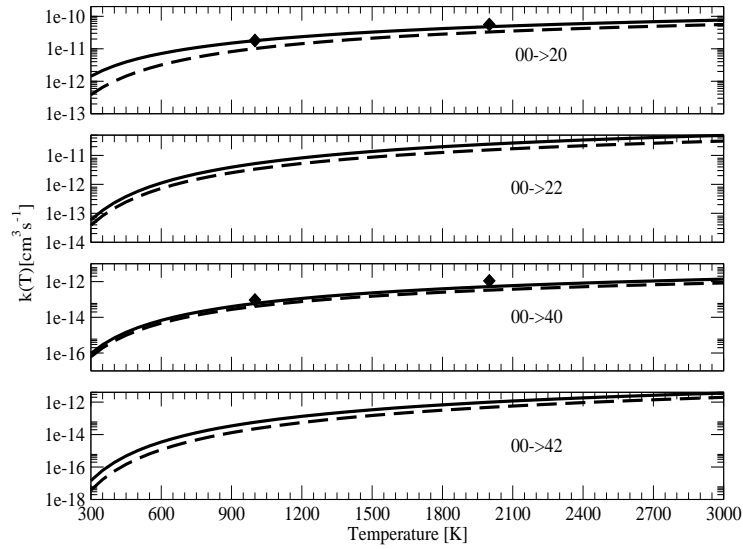


Figure 3. Temperature dependence of the state-resolved thermal rate constants for the $j_1 = j_2 = 0 \rightarrow j'_1 = 2, j'_2 = 0, j'_1 = 2, j'_2 = 2, j'_1 = 4, j'_2 = 0$ and $j'_1 = 4, j'_2 = 2$. The results for the DJ and BMKP PESs are given in solid and dashed lines, respectively. The diamonds are the theoretical data of work [16].

Table 3

Rate coefficients $k_{00 \rightarrow jj'}(T)$ (cm^3s^{-1}) calculated with the DJ PES for rotational transitions $00 \rightarrow 02, 22$ and 40 in comparison with other theoretical [15] and experimental [23] data.

$T(K)$	$k_{00 \rightarrow 20}$			$k_{00 \rightarrow 22}$		$k_{00 \rightarrow 40}$
	This work	[15]	[23]	This work	[15]	This work
50	6.25(-17)		1.1 \pm 0.1 (-16)	1.71(-22)		
60	3.80(-16)	4.4(-16)	6.0 \pm 0.7 (-16)	6.42(-21)	6.9(-21)	
100	1.64(-14)	1.6(-14)	2.2 \pm 0.4 (-14)	1.13(-17)	0.97(-17)	1.20(-22)
110	2.82(-14)		3.6 \pm 0.6 (-14)	3.26(-17)		6.89(-22)
120	4.47(-14)			8.02(-17)		3.01(-21)
150	1.28(-13)	1.2(-13)		6.16(-16)	4.5(-16)	8.14(-20)
200	3.98(-13)			5.37(-15)		2.48(-18)
300	1.43(-12)			5.94(-14)		9.59(-17)

Numbers in parentheses are powers of 10.

rotational inelasticity is dominated by the $00 \rightarrow 20$ transition.

The integral cross sections for an elastic $p\text{-H}_2 + p\text{-H}_2$ collision computed with both PESs are depicted in Fig. 2. The two cross sections are in reasonable agreement over a wide range of energies. Again the BMKP PES generates higher values. The difference becomes even larger at lower kinetic energies. In the figure we also provide experimental data from work [6]. The theoretical and the experimental results are in reasonable agreement with each other. This fact indicates, that the spherical parts of BMKP and DJ PESs are close in shape, which is a very important attribute for PESs.

The differences in the cross sections between the two potentials are also reflected in the state-resolved thermal rate constants, as shown in Fig. 3. Again, the BMKP PES underestimates the rate constant for the $00 \rightarrow 20$ transition, and overestimates those transitions of higher rotational levels. The near perfect agreement for the $00 \rightarrow 40$ transition is likely accidental. Because of the highly averaged nature of the rate constant, the difference is not as conspicuous as in the cross sections. We have also plotted in the same figure the rate constants reported previously in work [15], where Schwenke's PES [10] was used.

Finally, our rate constants for $00 \rightarrow 20, 22, 40$ rotational transitions calculated with the DJ PES at lower temperatures are listed in Table 3 together with the theoretical calculations of Flower et al. [15] and recent experimental results from work [23]. As can be seen our rate constants $k_{00 \rightarrow 20}(T)$ and $k_{00 \rightarrow 22}(T)$ are close to those of work [15]. The experimental results are higher by about 60% for 50 K and 30 % for 110 K.

4. SUMMARY and CONCLUSIONS

A systematical study of the state-resolved rotational excitation cross sections and rates in molecular *para*-/*para*-hydrogen collisions is completed. A test of convergence and the results for cross sections and rate coefficients using two different potential energy surfaces for the $\text{H}_2 - \text{H}_2$ system have been obtained for a wide range of kinetic energies.

Although our calculations revealed, that both PESs can provide the same type of behaviour in regard to cross sections and rates, there are still significant differences. The DJ potential overestimates by about 20-40 % the results at even relatively larger kinetic energies. This is especially true in regard to $00 \rightarrow 20$ rotational transition, where significant differences at around 300 K are seen in Fig. 3.

Considering the results of these calculations one can conclude that subsequent work is needed to further improve the H_2-H_2 PES. Detailed calculations including rotational-vibrational basis set and comparative analyses using both potentials at low and very low kinetic energies for o - H_2/o - H_2 and p - H_2/o - H_2 excitation-deexcitation collision processes currently are in progress in our group.

Acknowledgments

This work was supported by the St. Cloud State University internal grant program, St. Cloud, MN (USA).

REFERENCES

1. H. Rabitz, J. Chem. Phys., 57, (1972) 1718.
2. J.M. Farrar, Y.T. Lee, J. Chem. Phys., 57 (1972) 5492.
3. G. Zarur, H. Rabitz, J. Chem. Phys., 60 (1974) 2057
4. S.-I. Chu, J. Chem. Phys., 62, (1975) 4089.
5. S. Green, J. Chem. Phys., 62 (1975) 2271; J. Chem. Phys., 67 (1977) 715.
6. W. Bauer, B. Lantzsch, J.P. Toennies, K. Walaschewski, Chem. Phys. 17 (1976) 19.
7. T.G. Heil, S. Green, D.J. Kouri, J. Chem. Phys., 68 (1978) 2562.
8. L. Monchick, J. Schaefer, J. Chem. Phys., 73 (1980) 6153.
9. G. Danby, D.R. Flower, T.S. Monteiro, Mon. Not. R. Astr. Soc., 226 (1987) 739.
10. D.W. Schwenke, J. Chem. Phys., 89 (1988) 2076.
11. D.W. Schwenke, J. Chem. Phys., 92 (1990) 7267.
12. J. Schaefer, Astron. Astrophys. Suppl. Ser., 85 (1990) 1101.
13. A.I. Boothroyd, W.J. Keogh, P.G. Martin, M.J. Peterson, J. Chem. Phys., 95 (1991) 4331.
14. A. Aguado, C. Suarez, M. Paniagua, J. Chem. Phys., 101 (1994) 4004.
15. D.R. Flower, Mon. Not. R. Astron. Soc., 297 (1998) 334.
16. D.R. Flower, E. Roueff, J. Phys. B: At. Mol. Opt. Phys., 31 (1998) 2935.
17. V.A. Zenevich, G. D. Billing, J. Chem. Phys., 111 (1999) 2401.
18. D.R. Flower, J. Phys. B: At. Mol. Opt. Phys., 33 (2000) L193.
19. S.K. Pogrebnya, D.C. Clary, Chem. Phys. Lett., 363 (2002) 523.
20. S.Y. Lin, H. Guo, J. Chem. Phys., 117 (2002) 5183.
21. M.E. Mandy, S.K. Pogrebnya, J. Chem. Phys., 120 (2004) 5585.
22. M. Bartolomei, M.I. Hernandez, J. Campos-Martinez, J. Chem. Phys., 122 (2005) 064305.
23. B. Mate, F. Thibault, G. Tejeda, J.M. Fernandez, S. Montero, J. Chem. Phys., 122 (2005) 064313.
24. R.J. Hinde, J. Chem. Phys., 122 (2005) 144304.
25. A. Züttel, Naturwissenschaften, 91 (2004) 157.
26. J.E. Dove, A.C.M. Rusk, P.H. Cribb, P.G. Martin, Astrophys. J., 318 (1987) 379.
27. K.W. Hodapp, C.J. Davis, Astrophys. J., 575 (2002) 291.
28. G. Shaw, G.J. Ferland, N.P. Abel, P.C. Stancil, P.A.M. van Hoof, Astrophys. J. 624 (2005) 794.
29. R.A. Sultanov, N. Balakrishnan, Astrophys. J. 629 (2005) 305.
30. P. Diep, J.K. Johnson, J. Chem. Phys., 113 (2000) 3480; *ibid.* 112 (2000) 4465.
31. A.I. Boothroyd, P.G. Martin, W.J. Keogh, M.J. Peterson, J. Chem. Phys., 116 (2002) 666.
32. J.M. Hutson, S. Green, MOLSCAT VER. 14 (1994) (Distributed by Collabor. Comp. Proj. 6, Daresbury Lab., UK, Eng. Phys. Sci. Res. Council, 1994)